

Title	Ultra-soft magnetic Co-Fe-B-Si-Nb amorphous alloys for high frequency power applications
Authors	Ackland, Karl;Masood, Ansar;Kulkarni, Santosh;Stamenov, Plamen
Publication date	2018
Original Citation	Ackland, K., Masood, A., Kulkarni, S. and Stamenov, P. (2018) 'Ultra-soft magnetic Co-Fe-B-Si-Nb amorphous alloys for high frequency power applications', AIP Advances, 8(5), 056129 (7pp). doi: 10.1063/1.5007707
Type of publication	Article (peer-reviewed)
Link to publisher's version	https://aip.scitation.org/doi/10.1063/1.5007707 - 10.1063/1.5007707
Rights	© 2018, the Author(s). Published by AIP Publishing. All article content, except where otherwise noted, is licensed under a Creative Commons Attribution (CC BY) license (http://creativecommons.org/licenses/by/4.0/). - http://creativecommons.org/licenses/by/4.0/
Download date	2025-04-23 01:16:37
Item downloaded from	https://hdl.handle.net/10468/5927



UCC

University College Cork, Ireland
Coláiste na hOllscoile Corcaigh

Ultra-soft magnetic Co-Fe-B-Si-Nb amorphous alloys for high frequency power applications

Karl Ackland, Ansar Masood, Santosh Kulkarni, and Plamen Stamenov

Citation: *AIP Advances* **8**, 056129 (2018); doi: 10.1063/1.5007707

View online: <https://doi.org/10.1063/1.5007707>

View Table of Contents: <http://aip.scitation.org/toc/adv/8/5>

Published by the [American Institute of Physics](#)

Articles you may be interested in

[Structure and soft magnetic properties of Fe-Si-B-P-Cu nanocrystalline alloys with minor Mn addition](#)

AIP Advances **8**, 056110 (2018); 10.1063/1.5007109

[Dual-color short-wavelength infrared photodetector based on InGaAsSb/GaSb heterostructure](#)

AIP Advances **8**, 025015 (2018); 10.1063/1.5020532

[Mechanical stress relaxation in adhesively clamped carbon nanotube resonators](#)

AIP Advances **8**, 025118 (2018); 10.1063/1.5020704

[Numerical simulations to model laser-driven coil-capacitor targets for generation of kilo-Tesla magnetic fields](#)

AIP Advances **8**, 025103 (2018); 10.1063/1.5019219

[Influence of La-Mn substitutions on magnetic properties of M-type strontium hexaferrites](#)

AIP Advances **8**, 056235 (2018); 10.1063/1.5007695

[New Fe-based soft magnetic alloys composed of ultrafine grain structure](#)

Journal of Applied Physics **64**, 6044 (1988); 10.1063/1.342149

HAVE YOU HEARD?

Employers hiring scientists and
engineers trust

PHYSICS TODAY | JOBS

www.physicstoday.org/jobs



Ultra-soft magnetic Co-Fe-B-Si-Nb amorphous alloys for high frequency power applications

Karl Ackland,¹ Ansar Masood,² Santosh Kulkarni,² and Plamen Stamenov^{1,a}

¹*School of Physics and CRANN, Trinity College, Dublin 2, Ireland*

²*ICT for Energy Efficiency, Microsystems Center, Tyndall National Institute, University College Cork, Cork, Ireland*

(Presented 10 November 2017; received 2 October 2017; accepted 29 January 2018; published online 14 February 2018)

With the continuous shrinkage of the footprint of inductors and transformers in modern power supplies, higher flux, while still low-loss metallic replacements of traditional ferrite materials are becoming an intriguing alternative. One candidate replacement strategy is based on amorphous CoFeBSi soft-magnetic alloys, in their metallic glass form. Here the structural and magnetic properties of two different families of CoFeBSi-based soft magnetic alloys, prepared by arc-melting and subsequent melt spinning (rapid quenching) are presented, targeting potential applications at effective frequencies of 100 kHz and beyond. The nominal alloy compositions are $\text{Co}_{67}\text{Fe}_4\text{B}_{11}\text{Si}_{16}\text{Mo}_2$ representing commercial Vitrovac and $\text{Co}_{72-x}\text{Fe}_x\text{B}_{28-y}$ (where B includes non-magnetic elements such as Boron, Silicon etc. x varies between 4 and 5 % and y is varied from 0 to 2 %) denoted Alloy #1 and prepared as a possible higher performance alternative, i.e. lower power loss and lower coercivity, to commercial Vitrovac. Room temperature magnetization measurements of the arc-melted alloys reveal that compared to Vitrovac, Alloy #1 already presents a ten-fold decrease in coercivity, with $H_c \sim 1.4 \text{ Am}^{-1}$ and highest figure of merit of $(M_s/H_c > 96)$. Upon melt-spinning the alloys into thin ($< 30 \mu\text{m}$) ribbons, the alloys are essentially amorphous when analyzed by XRD. Magnetization measurements of the melt-spun ribbons demonstrate that Alloy #1 possesses a coercivity of just 2 Am^{-1} , which represents a significant improvement compared to melt-spun ribbons of Vitrovac (17 Am^{-1}). A set of prototype transformers of approximately 10 turns of Alloy #1 ribbon exhibits systematically $H_c < 10 \text{ Am}^{-1}$ at 100 kHz, without a noticeable decrease in coupled flux and saturation. © 2018 Author(s). All article content, except where otherwise noted, is licensed under a Creative Commons Attribution (CC BY) license (<http://creativecommons.org/licenses/by/4.0/>). <https://doi.org/10.1063/1.5007707>

I. INTRODUCTION

Lower power loss and higher flux replacements for traditional ferrite based inductors are required with the continuous shrinking of inductor footprint. One candidate replacement strategy is based on the amorphous CoFeBSi soft-magnetic systems in their metallic glasses forms. This is enabled by significant advancements by the power semiconductor industry of faster and efficient power switches, as the requirements for smaller and more efficient magnetic components becomes more imminent, at these higher frequencies.² One of the main difficulties in the miniaturization of power conversion circuits is the reduction in size of energy storage and transfer devices, i.e. inductors and transformers.³ These essential components normally occupy a significant fraction of volume ($\sim 30\%$) of the power converters. Inductors and transformers typically use a magnetic core to store the energy. A key roadblock in advancing the passive component technology is the low flux density provided

^aCorresponding author: Plamen Stamenov (e-mail: plamen.stamenov@tcd.ie).

by ferrite-based magnetic core materials. Over the last decade, there has been significant research focused on developing alternate high flux density soft magnetic materials to replace bulky and large ferrite-based solutions.² Excellent soft magnetic properties and high electrical resistivity are both prerequisites for the development and the use of these magnetic materials in high-frequency applications (> 100 kHz).¹

Alternative high magnetic flux density materials are amorphous metals which are optimized for high electrical resistivity ($\sim 150 \mu\Omega\text{cm}$), at least 3 times higher resistivity than silicon steel.^{2,3} This novel class of materials realizes a viable combination of excellent soft magnetic, mechanical and corrosion properties owing to their unique disordered atomic structure. In this work, we present the Co-Fe-B-Si-Nb based soft-magnetic amorphous alloy system and their potential use in inductor applications at and above 100 kHz.

Here the structural and magnetic properties of two different CoFeBSi based soft-magnetic alloys prepared by arc-melting and subsequent melt spinning (rapid quenching) are studied, for potential use in inductor applications at 100 kHz. The nominal alloy compositions were $\text{Co}_{67}\text{Fe}_4\text{B}_{11}\text{Si}_{16}\text{Mo}_2$ representing commercial Vitrovac¹ and $\text{Co}_{72-x}\text{Fe}_x\text{B}_{28}$ (where B includes non-magnetic elements such as Boron, Silicon etc.) representing Alloy #1 and prepared as a possible higher performance alternative, i.e. lower power loss and lower coercivity, to commercial Vitrovac.

II. EXPERIMENTAL METHOD

The nominal alloy compositions are $\text{Co}_{72-x}\text{Fe}_x\text{B}_{28}$ (where B includes non-magnetic elements such as Boron, Silicon etc.) represented as Alloy #1. First, the desired quantities of each element are weighed out using a standard microbalance to a precision of ~ 0.2 mg. The starting materials are: Co pieces 99.5 % trace metals basis (TMB), Fe chips 99.98% (TMB), Boron crystalline pieces 99.7 % TMB, and Si pieces 99.95 % TMB, all sourced from Sigma Aldrich. The remaining non-magnetic elements used have a nominal purity of at least 99.8 % TMB.

The alloys are prepared by arc-melting in high purity argon. Heating up to ~ 4000 K occurs from an electric arc, which is created between a copper electrode and sharp welding tip (2 % thoriated red-tungsten). The elements to be melted are contained within a water-cooled copper hearth. In general, the lower melting point elements are placed under those of higher melting point, with the exception of boron, which is placed at the bottom of the hearth and an adjusted excess added so as to retain stoichiometry. The ingots are flipped and re-melted four times to ensure homogeneity and a uniform luster. High purity titanium is used as a getter for oxygen. Typical ingot masses are ~ 1 gram. Part of the ingots are then cut, mounted in acrylic resin and cured, enabling subsequent surface polishing using sequentially finer grades of sandpaper and lapping paper (5, 1 and $0.3 \mu\text{m}$) respectively.

X-Ray powder diffraction (XRD) data of the arc-melted polished ingots are collected using a Phillips PANalytical X'pert Pro diffractometer with an operational wavelength of 1.5405 \AA (Cu K_α anode), while micrographs are obtained by Scanning Electron Microscopy (SEM), using a Zeiss Ultra field emission microscope, with additional elemental detection (EDX) using an Oxford instruments X-Max EDX silicon drift detector to check qualitative elemental composition.

Ribbons are subsequently produced by induction melting and melt-spinning the arc-melted ingots (in 1 gram batches) at ambient pressure and atmosphere. An argon jet (at an overpressure of 1 bar) is used to eject the molten liquid contained in a quartz vial. Typical experimental parameters and conditions used are: quartz vial of 60 mm length, 8 mm inner diameter and 0.2 mm diameter orifice, a starting ingot mass of 1 gram, a nozzle to wheel angle of 20 degrees from the perpendicular, a nozzle to wheel separation of ~ 1 mm, a wheel diameter of 90 mm and a wheel speed of 50-210 m/s. Using the above general conditions ribbons of $\sim 20 \mu\text{m}$ thickness, ~ 6 metres total length (with maximum individual discrete ribbon lengths of up to 10 cm) and ~ 1 mm width are obtained.

A superconducting quantum interference device magnetometer (SQUID, MPMS XL5), is used to measure the in-plane saturation magnetization of the as-produced ribbons at room temperature in a magnetic induction range of ± 5 T. The ribbon samples are mounted on long diamagnetic PE straws.

Data are collected, at the maximum gradient point of the second derivative response curve, with no auto-tracking. The very-small coercivity ($< 5 \text{ Am}^{-1}$) characteristic of the ribbons is more accurately measured by B-H loop tracer, than by SQUID magnetometry, hence H_c was measured by a custom BH-looper (at the Tyndall National Institute).

Ribbon thickness and surface structure are quickly and approximately determined by optical microscopy, using a Nikon Eclipse L150 microscope, typically using 100x magnification.

The power loss characterization setup includes series 8200 power supply from Global Specialties as signal generator, power amplifier from Applied Research, Agilent N2775A current sensor, and Tektronix TPS 2014 oscilloscope. The amorphous ribbons are shaped into toroidal cores and ~ 5 turns of material are utilized. The inner and outer diameter of the core are 5.5 mm and 6 mm, respectively. For transformer style measurements, 25 turns of copper wire are wound around the core as primary and secondary coils. An air core transformer with same dimensions is also prepared and used in a normalization experiment, in order to eliminate the influence of the air coupling. The details of the instrument and the equivalent circuit are published in our previous work.¹

III. RESULTS AND DISCUSSION

XRD data acquired from the polished faces of the arc-melted ingots are shown in Figure 1. Vitrovac has a hexagonal close-packed (hcp) crystal structure, with some indexed hcp Cobalt also detected, and overlapping the hcp Vitrovac phase. No other phases are detected. Alloy #1 has a

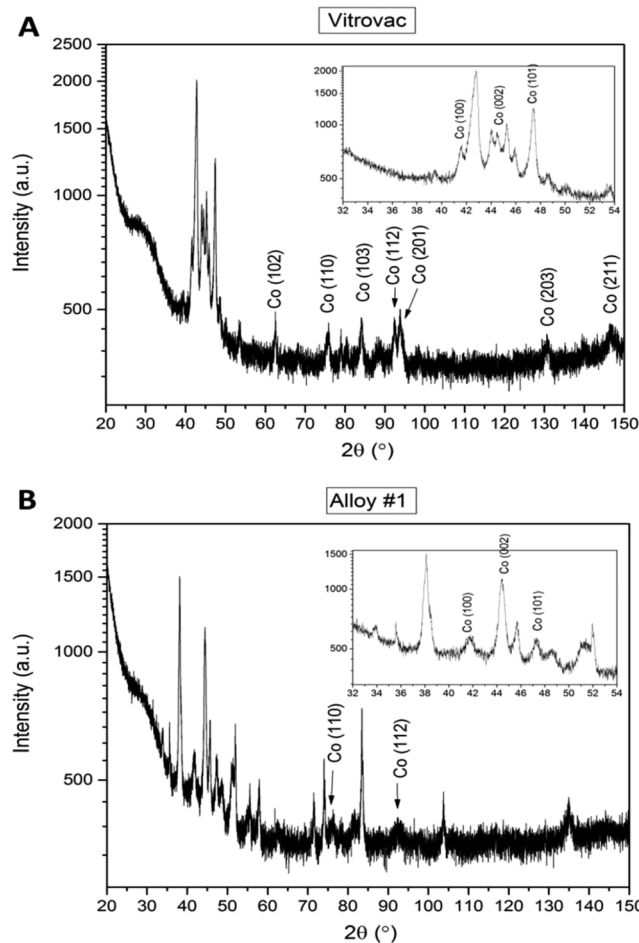


FIG. 1. XRD profiles of arc-melted polished ingots of (a) Vitrovac and (b) Alloy #1.

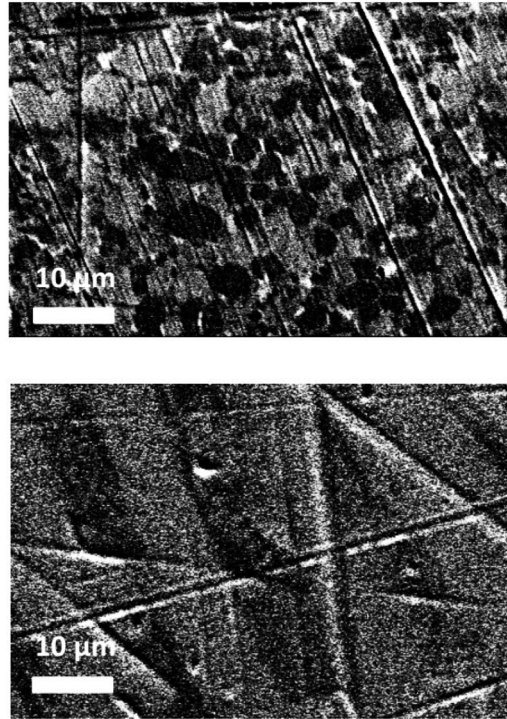


FIG. 2. Micrographs of the arc-melted polished ingots of Vitrovac and Alloy #1.

face-centred cubic (fcc) crystal structure; some additional hcp Cobalt was detected, which overlaps the fcc Alloy #1 phase, but less than that measured in Vitrovac. No other phases are detected. The crystal structures of both alloys determined by XRD are in agreement with the binary phase diagrams for the respective compositions.

Micrographs of the polished alloy surface (Figure 2) reveal that whereas Vitrovac possesses a granular morphology, Alloy #1 is eutectic lamellar.

Room temperature magnetization measurements of the arc-melted alloys reveal, that compared to Vitrovac, Alloy #1 already presents a ten-fold decrease in coercivity, with $H_c \sim 1.4 \text{ kAm}^{-1}$. Upon melt-spinning the alloys into thin ($< 40 \mu\text{m}$) ribbons, magnetization measurements (Figure 3) showed

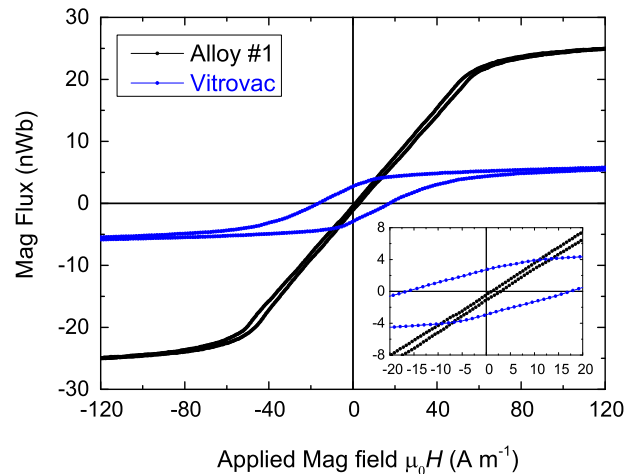


FIG. 3. Room temperature magnetization curves of melt-spun ribbons of Vitrovac and Alloy #1.

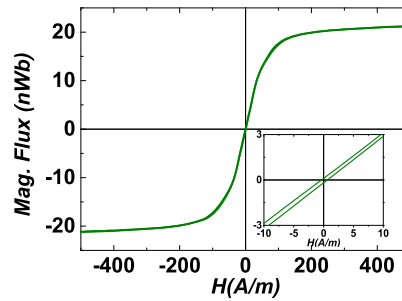


FIG. 4. in-Plane BH-loop of the B= 24% amorphous ribbon measured by BH-loop tracer. Inset represents the low magnetic field behaviour of the same sample.

that Alloy #1 possessed a coercivity of just 2 Am^{-1} , which again represents a significant improvement compared to melt-spun ribbons of Vitrovac (17 Am^{-1}). Furthermore, a prototype transformer, of 10 turns of Alloy #1 ribbon, exhibits $H_c < 10 \text{ A m}^{-1}$ at 100 kHz (Figure 4), the chosen frequency of merit for applications.

The coercivity of the amorphous ribbons is measured on BH -loops along the axis of the ribbons and presented in Fig. 5. In general, amorphous materials exhibit low coercivity and high permeability. The low coercivity is essentially due to the absence of magnetocrystalline and magnetoelastic anisotropies.^{2,4} The saturation magnetization (shown on figure 6) drops, as expected, due to the dilution of the main magnetic component of the alloys. As this drop affects the performance of the alloys in a detrimental fashion, it is advisable to use a figure of merit (for example M_s/H_c) to look for an indication of optimal performance. The same is shown on figure 7 for the same compositional range. There is a clear and well-pronounced maximum of the figure of merit in the vicinity of 24 % B content.

Figure 8 shows the power loss density, $P(B)$, at different peak magnetic flux density at $f = 100 \text{ kHz}$. The power loss density is measured at $3\text{-}100 \text{ kW/m}^3$ at a peak induction of 1 T, for $\sim 20 \mu\text{m}$ amorphous ribbons containing B=19-30%. The impact of H_c on the high frequency soft magnetic properties is clearly reflected. The power loss density in a magnetic material has three main contributions: the hysteresis loss, the classical eddy current loss and the excess loss. The total loss is dominated by the sum of all these three types of losses, but their frequency dispersions vary and the optimization of a material composition can only be performed in the context of a particular

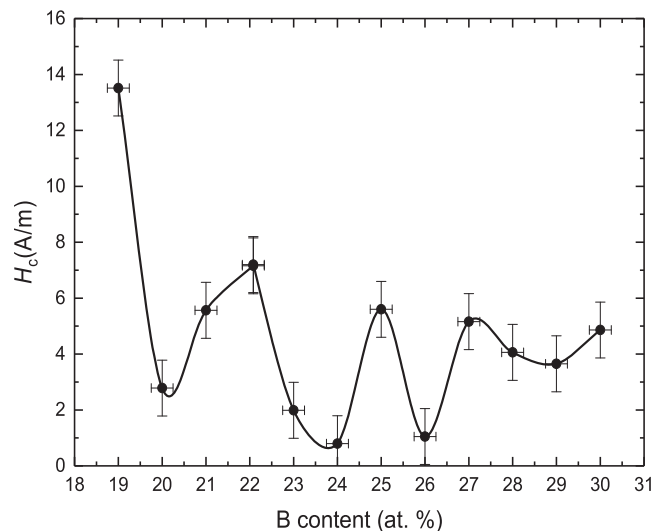


FIG. 5. Coercivity (H_c) of the amorphous ribbons as a function of B (%). The line is just a guide to the eye.

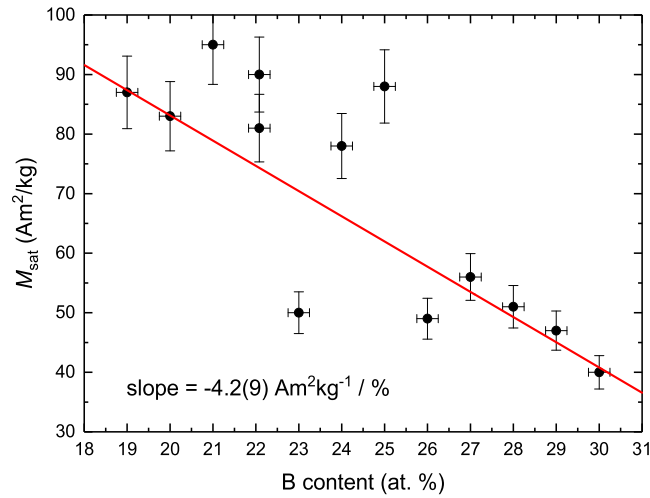


FIG. 6. Saturation magnetization (M_{sat}) vs. Boron content (at. %) and the expected linear dependence (within this narrow interval of compositions).

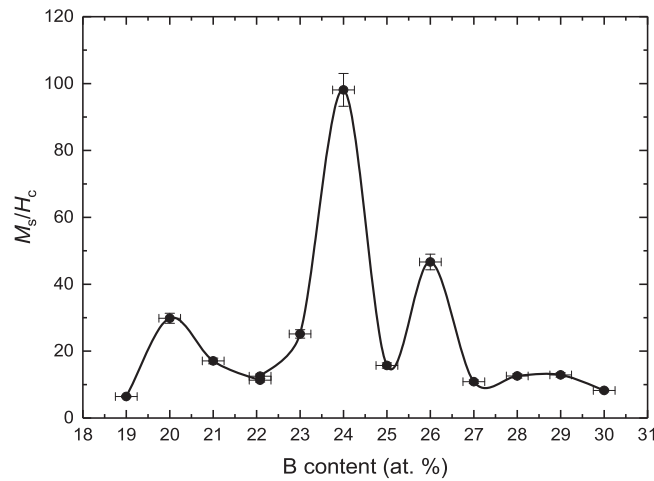


FIG. 7. Figure of merit (M_{sat}/H_c) vs. Boron content (at. %). The line is a guide to the eye. The x-error bars are based on maximal boron loss possible.

target frequency region, operational temperature, peak flux density, static magnetic bias, etc. Here, we focus on close to room temperature operation, with peak magnetic induction below saturation values.

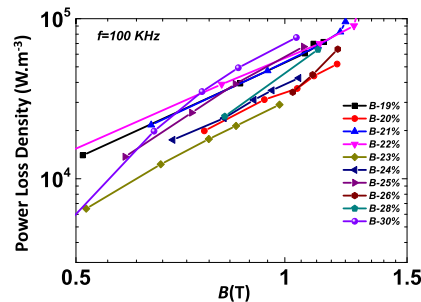


FIG. 8. The powerless density of the amorphous measured at 100 KHz for alloys containing different concentration of B.

IV. CONCLUSIONS

The preparation of a series of soft-magnetic melt-spun ribbons and transformer test cores has been presented. The results indicate significant performance advantages in terms of flux density and loss minimization for compositions with B~ 24 %, in a fashion similar to other far more Fe-rich systems.⁵ This is due to the stabilization of local order corresponding to or derived via amorphisation from fcc long-range order. This minimizes the amount of hexagonal Co (and other ordered hcp impurity phases) inclusions and minimizes the potential obstacles for domain rotation and domain-wall propagation, and correspondingly drives the coercivity down. In view of the possibilities for further in-situ and ex-situ thinning of melt-spun ribbons for the minimization of eddy current losses, mechanical or laser scoring and hard-magnetic biasing, for the minimization of the hysteresis losses, the above compositional family should also offer routes to target applications at higher frequencies in the range 100 – 500 kHz.

ACKNOWLEDGMENTS

This project is co-funded by the European Regional Development Fund (ERDF) under Ireland's European Structural and Investment Funds Programme 2014-2020. Funding from the Enterprise Ireland Commercialization Fund (EI-CF/2016) for the "Premium Magnetic Components for High Efficiency Power Supplies" (PreMag) project is gratefully acknowledged. S. Kulkarni also gratefully acknowledges funding from the Science Foundation Ireland (SFI) Starting Investigator Research Grant (SIRG). P. Stamenov would also like to acknowledge support received under the AMBER (SFI-funded) research center.

¹ *Amorphous Metals VITROVAC (1989) Catalogue*, Edition 7 (Vacuumschmelze GmbH, Hanau, Germany).

² S. Kulkarni *et al.*, "Low loss magnetic thin films for off-line power conversion," *IEEE Transactions on Magnetics* **50**(4) (2014).

³ A. Masood *et al.*, "Effect of Ni-substitution on glass forming ability, mechanical, and magnetic properties of FeBNbY bulk metallic glasses," *Journal of Applied Physics* **113**(1) (2013).

⁴ G. Herzer, "Modern soft magnets: Amorphous and nanocrystalline materials," *Acta Materialia* **61**(3), 718–734 (2013).

⁵ S. Lee *et al.*, "Magneto-thermo-gravimetric technique to investigate the structural and magnetic properties of Fe-B-Nb-Y bulk metallic glass," 13th International Conference on Rapidly Quenched and Metastable Materials, 2009. 144.